Decaying light particles in the SHiP experiment: Signal rate estimates for hidden photons

D. Gorbunov,[1,2,*] A. Makarov,[1,†] and I. Timiryasov[1,3,‡]

[1] *Institute for Nuclear Research of the Russian Academy of Sciences, Moscow 117312, Russia*
[2] *Moscow Institute of Physics and Technology, Dolgoprudny 141700, Russia*
[3] *Physics Department, Moscow State University, Vorobievy Gory, Moscow 119991, Russia*

For the extension of the Standard Model with light hidden photons we present preliminary estimates of the signal rate expected at the recently proposed fixed target SHiP experiment exploiting the CERN SPS beam of 400 GeV protons.

arXiv:1411.4007v2 [hep-ph] 26 Feb 2015

I. INTRODUCTION: THE EXPERIMENT AND THE MODEL TO BE TESTED

Unsolved phenomenological problems—neutrino oscillations, dark matter phenomena, baryon asymmetry of the Universe—definitely ask for an extension of the Standard Model of particle physics (SM). It is natural to find the corresponding new particles at a mass scale not much higher than the electroweak scale. Otherwise the hierarchy problem arises in the scalar sector: quantum corrections of heavy particles push the SM Higgs boson mass up to their mass scale. While the LHC scrutinizes thoroughly the (sub-)TeV scale, there is a logical possibility of having thus far elusive new physics at a (much) lower scale. The absence of any direct evidence of the new physics may be attributed to the weakness of interaction between known and new particles. In the search for such new physics the superior experiments are those operating on the high-intensity frontier.

An example of this type of experiment is SHiP (Search for Hidden Particles [1]), the recently proposed [2] new fixed target experiment at the CERN SPS 400 GeV proton beam. The original motivation [3] was to search for $\mathcal{O}(1)$ GeV sterile neutrinos of νMSM, one of the most economic extensions of the SM capable of explaining all the three aforementioned phenomenological problems with only three new fields (singlet with respect to SM gauge groups fermions) added to the SM, see [4] for review. Mixing between singlet fermions and active neutrinos is responsible for both the singlet production in decays of heavy mesons (generated by protons on target) and subsequent singlet decays into SM particles (the main signature for the SHiP detector), see [5] for details. The flux of secondary particles from proton scatterings is suppressed by the very dense (tungsten) dump placed downstream. The main idea is to have a large detector ($5\times5\,\mathrm{m}^2\times50\,\mathrm{m}$ [2]) and place it as close to the target as possible (at a distance of about 60 m [2]) in order to maximize the number of potential singlet decays within the detector fiducial volume and still have the background under control. This makes SHiP *a universal tool to probe any new physics which introduces sufficiently light and long-lived particles produced by protons on target and then decaying into SM particles.*

In this paper we consider one of the examples of such new physics, which provides long-lived light particles that can be searched for at SHiP, specifically models with massive hidden photons. The SM Lagrangian $\mathcal{L}_{SM}$ is extended in the following way:

$$\mathcal{L} = \mathcal{L}_{SM} - \frac{1}{4}F'_{\mu\nu}F'^{\mu\nu} + \frac{\epsilon}{2}F'_{\mu\nu}F^{\mu\nu} + \frac{m^2_{A'}}{2}A'_\mu A'^\mu, \quad (1)$$

where A'_μ is massive gauge field of a new (dubbed dark) $U'(1)$ group, $F'_{\mu\nu} \equiv \partial_\mu A'_\mu - \partial_\nu A'_\mu$, and ϵ is parameter of kinetic mixing. The mixing provides effective coupling between A' and pairs of the SM charged particles, which determines the model's phenomenology. Present phenomenological limits on ϵ and $m_{A'}$ are shown in Fig. 1. Hidden photon may be a messenger of the hidden sector,

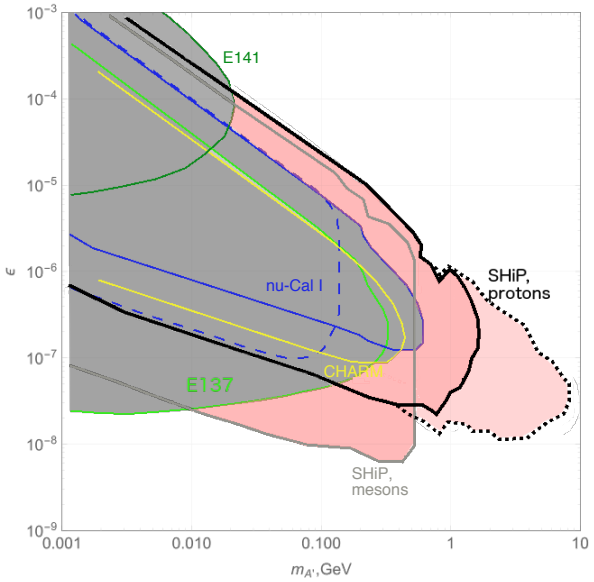

FIG. 1. Excluded regions in the hidden photon model parameter space (see [6–8] for details), the pink regions are expected from SHiP. Two estimates of proton contribution, with (solid line) and without (dotted line) accounting for the proton form factor, are presented. The correct line goes in between, see Sec. II A.

that is responsible for (some of) the unsolved problems

* gorby@ms2.inr.ac.ru
† a.mr@mail.ru
‡ timiryasov@inr.ac.ru

we started with (see e.g. [9] for dark matter). The purpose of this work is to estimate the number of hidden photon decays inside the SHiP detector. This is the first step towards the estimate of the SHiP sensitivity to models with hidden photons, which in order to be completed, requires fixing the experiment layout, understanding the detection efficiency, and calculating the expected background.

II. PRODUCTION MECHANISMS

Hidden photons can be produced directly, via proton (quark) or lepton bremsstrahlung, and indirectly, in meson decays. The relevant leptons and mesons are secondary particles produced either at proton scattering off target or when the hadron and lepton cascades, initiated by scattering, propagate in the dump material.

A. Proton bremsstrahlung

In a fixed target experiment, particles A' are generated by scattering protons through a process analogous to ordinary photon bremsstrahlung. Consider a proton of mass m_p with initial 3-momentum P and initial energy E_p. Let $E_{A'}$ be the energy of A' and z denote a fraction of the momentum P carried away by A' in the direction of incoming proton. Therefore $P\cdot z = p_\parallel$, $p_\parallel$ and $\overrightarrow{p}_\perp$ are longitudinal and transverse components of A' 3-momentum $P_{A'}$. The differential A'-production rate per proton interaction, calculated in the Weizsäcker-Williams approximation, reads [8]

$$\frac{dN}{dz dp_\perp^2} = \frac{\sigma_{pA}(s')}{\sigma_{pA}(s)}\, w_{ba}(z, p_\perp^2)\,, \tag{2}$$

where $s' = 2m_p(E_p - E_{A'})$, $s = 2m_p E_p$ and

$$w_{ba}(z,p_\perp^2) = \frac{\epsilon^2\alpha_{QED}}{2\pi H}\left[\frac{1+(1-z)^2}{z}\right.$$
$$-2z(1-z)\left(\frac{2m_p^2+m_{A'}^2}{H} - z^2\frac{2m_p^4}{H^2}\right)$$
$$\left.+2z(1-z)(z+(1-z)^2)\frac{m_p^2 m_{A'}^2}{H^2} + 2z(1-z)^2\frac{m_{A'}^4}{H^2}\right]$$

with $H(p_\perp^2, z) = p_\perp^2 + (1-z)m_{A'}^2 + z^2 m_p^2$ and fine structure constant $\alpha_{QED} \approx 1/137$. The hadronic cross section is factorized and related to the proton-proton scattering cross section σ_{pp} as $\sigma_{pA}(s) = f(A)\sigma_{pp}(s)$ with function $f(A)$ depending only on atomic number A. Thus, it drops out in expression (2) for the event rate. For inelastic proton-proton cross section we use the fit from [10].

Equation (2) was originally derived [11] under a set of specific conditions. For a beam-dump-type experiment these conditions could be summarized as follows [8]:

$$E_p,\, E_{A'},\, E_p - E_{A'} \gg m_p,\, m_{A'},\, \sqrt{p_\perp^2}. \tag{3}$$

Another restriction comes from our treatment of scattering proton as an entire particle and not a bunch of partons: we consider the proton, but not quark, bremsstrahlung at high energies. To ensure that we are dealing with the entire proton, we restrict proton-nuclei momentum transfer, $(P - P_f - P_{A'})^2 < \Lambda_{QCD}^2$, where P_f denotes the 3-momentum of the outgoing proton. Then, we also require the 3-momentum of the produced A' to be inside a cone determined by a detector geometry (see Sec. IV A). We have checked numerically that the latter two restrictions guarantee the fulfillment of conditions (3). These two restrictions are summarized in the following function:

$$f(z, p_\perp^2) = \theta\left(\Lambda_{QCD}^2 - (P - P_f - P_{A'})^2\right)\cdot f_{\text{fiducial}}. \tag{4}$$

with f_{fiducial} referring to the restriction from the detector geometry. Finally, to obtain a number of A' whose trajectories cross the fiducial volume of detector one integrates eq. (2) with factor (4).

In the considerations above we neglected the proton internal structure, however, the momentum transfer for heavy A' emission can be sufficient to feel it. This effect can be addressed at the parton level, which we leave for future studies. Here, to be conservative, we restrict the kinematics to the region where details of the internal structure are not important, which is done by introducing the Dirac F_1 and Pauli F_2 form factors into the proton electric current (see, e.g. [12]):

$$J_\mu(p,p') = \bar{u}(p')\left(\gamma_\mu F_1(q^2) + \frac{1}{2m_p} i\sigma_{\mu\nu}q^\nu F_2(q^2)\right)u(p),$$

where $q = p - p'$ is the 4-momentum transfer. Then the production rate of A' (2) gets multiplied by $F_1^2(m_{A'}^2)$ (the contribution of F_2 can be neglected since $F_1(q^2)/F_2(q^2) \sim q^2$ for large q^2). In the simplest dipole parametrization the Dirac form factor has form $F_1 = (1 + q^2/m_D^2)^{-2}$ with $m_D^2 = 12/r_D^2$ being the Dirac mass squared and the Dirac radius $r_D \approx 0.8\,\text{fm}$ [13]. The dependence on q^2 refers to a recoil of other constituents that is redundant since, in fact, all final hadronic states contribute. Hence, introduction of the proton form factor leads to sufficient underestimate of the A' flux compared to the quark bremsstrahlung. *Given our restrictions we arrive at the conservative lower limit on the hidden photon flux.*

B. Secondary particles bremsstrahlung

Hidden photons can be created by secondary particles in the beam dump (tungsten, lead, etc.). The A'-production cross section in the electron bremsstrahlung process was calculated in [14] in the Weizsäcker-Williams

approximation. For an incoming electron of energy E_0, the differential cross section to produce A' of energy $E_{A'} \equiv xE_0$ is

$$\frac{d\sigma}{dx\, dcos\theta_{A'}} \approx \frac{8Z^2\alpha_{QED}^3\epsilon^2 E_0^2\, x}{U^2}\frac{\chi}{Z^2} \times \left[(1-x+x^2/2) - \frac{x\,(1-x)m_{A'}^2 E_0^2\, x\,\theta_{A'}^2}{U^2}\right], \quad (5)$$

where $\theta_{A'}$ is the angle in the lab frame between the emitted A' and the incoming electron, Z is the atomic number of the dump atoms,

$$U = U(x,\theta_{A'}) = E_0^2\, x\,\theta_{A'}^2 + m_{A'}^2\frac{1-x}{x} + m_e^2\, x, \quad (6)$$

and an effective flux of photons (emitted by a rapidly moving atom in the rest frame of incoming electron) is defined as follows:

$$\chi \equiv \int_{t_{min}}^{t_{max}} dt\,\frac{t-t_{min}}{t^2}\,G_2(t), \quad (7)$$

where $t_{min} = (m_{A'}^2/2E_0)^2$, $t_{max} = m_{A'}^2$ and $G_2(t) = G_{2,el}(t) + G_{2,in}(t)$ is a general electric form factor, the sum of elestic and inelastic parts (see [14] for details). To simplify numerical integration we neglect x- and $\theta_{A'}$-dependences of t_{min} in (7). This can lead [15] to an overestimate of the cross section by $\sim 30\%$, which only insignificantly affects our results for the SHiP discovery potential.

C. Production in meson decays

Hidden photon A' can emerge in meson electromagnetic decays (if kinematics admits) due to mixing with photon. For the corresponding branching ratio of π^0 meson decay, one has the following estimate [16]:

$$\mathrm{Br}(\pi^0 \to A'\gamma) \simeq 2\epsilon^2\left(1-\frac{m_{A'}^2}{m_{\pi^0}^2}\right)^3 \mathrm{Br}(\pi^0\to\gamma\gamma)\,. \quad (8)$$

There is a similar expression for η^0-meson with obvious replacement $\pi^0 \leftrightarrow \eta^0$ in (8).

For branching ratios of vector meson V (e.g., $V = \rho^\pm, \rho^0, \omega$) decays into A' and pseudoscalar meson P (e.g., $P = \pi^\pm, \pi^0, \pi^0$), one finds:

$$\mathrm{Br}(V^\pm \to PA') \simeq \epsilon^2 \times \mathrm{Br}(V^\pm \to P\gamma) \times \frac{(m_V^2 - m_{A'}^2 - m_P^2)^2\sqrt{(m_V^2 - m_{A'}^2 + m_P^2)^2 - 4m_V^2 m_P^2}}{(m_V^2 - m_{A'}^2)^3}, \quad (9)$$

where m_V is the mass of the decaying vector meson and m_P is the mass of the pseudoscalar meson.

We are interested only in the mesons with a sufficient decay branching ratio. Another obvious requirement is that those same mesons should be produced in sufficient quantities in the SHiP setup. Therefore, in what follows we account only for π^0 and η^0 contributions.

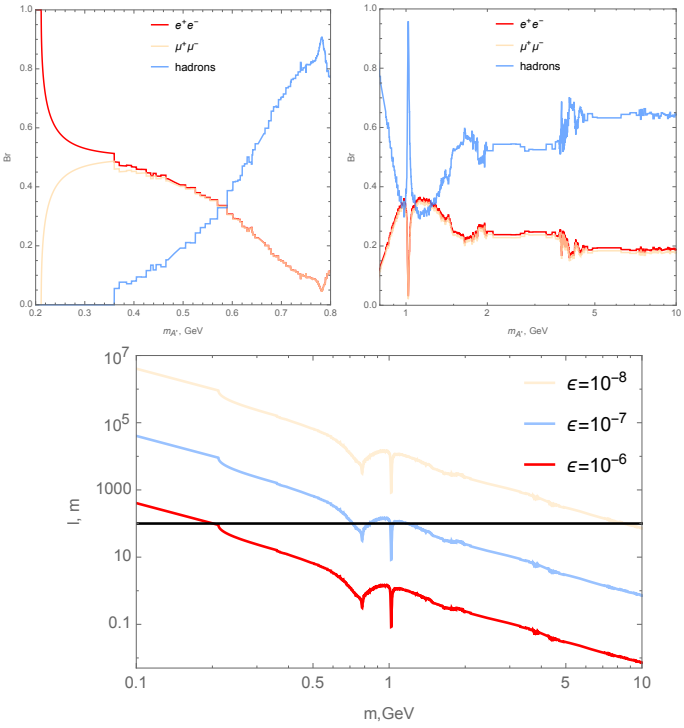

FIG. 2. *Top panels:* branching ratios of A' into e^+e^-, $\mu^+\mu^-$ and hadrons. *Bottom panel:* decay length of A' with energy 50 GeV; horizontal line represents the charachteristic length scale 100 m, particles of much shorter decay length do not reach SHiP detector.

III. HIDDEN PHOTON DECAY PATTERN

The photon-paraphoton mixing ϵ is responsible for hidden photon decays into pairs of charged SM particles. The partial decay width into a lepton pair is given by [8]

$$\Gamma_{A'}^{l^+l^-} = \frac{1}{3}\alpha_{\mathrm{QED}} m_{A'}\epsilon^2\sqrt{1-\frac{4m_l^2}{m_{A'}^2}}\left(1+\frac{2m_l^2}{m_{A'}^2}\right),$$

where m_l is the lepton mass. The partial decay width into hadrons can be estimated as

$$\Gamma_{A'}^{\mathrm{hadrons}} = \frac{1}{3}\alpha_{\mathrm{QED}} m_{A'}\epsilon^2\cdot R(m_{A'}), \quad (10)$$

where

$$R(\sqrt{s}) = \frac{\sigma(e^+e^-\to \mathrm{hadrons})}{\sigma(e^+e^-\to\mu^+\mu^-)} \quad (11)$$

is the energy- ($\sqrt{s}$-) dependent ratio [10]. Resulting branching ratios for the three relevant channels are shown in Fig.2.

Neglecting possible invisible decay modes (e.g., those associated with decay into hidden sector particles if they exist) one has the following for the total decay width:

$$\Gamma_{A'}^{\mathrm{tot}} = \Gamma_{A'}^{e^+e^-} + \Gamma_{A'}^{\mu^+\mu^-} + \Gamma_{A'}^{\mathrm{hadrons}}.$$

Thus the A' decay length reads (see also Fig. 2)

$$\gamma c\tau_{A'} = \frac{c\gamma}{\Gamma^{\rm tot}_{A'}}, \tag{12}$$

with the γ factor in the laboratory frame, $\gamma = E_{A'}/m_{A'}$.

IV. SIGNAL EVENT RATE

A. Hidden photon decays inside the SHiP detector

The probability for A' to decay inside the fiducial volume of the detector reads

$$w_{\rm det} \equiv w_{\rm det}(E_{A'}, m_{A'}, \epsilon) = \exp\left(-l_{\rm sh}/(\gamma(E_{A'})c\tau_{A'})\right) \times \left[1 - \exp\left(-l_{\rm det}/(\gamma(E_{A'})c\tau_{A'})\right)\right], \tag{13}$$

where $l_{\rm sh}$ is the muon shielding length (60 m for SHiP [2]) and $l_{\rm det}$ is the length of the detector fiducial volume (50 m).

The proposed fiducial volume of the SHiP detector is the 50 m-length cylindrical vacuum vessel of 5 m diameter. To estimate the expected number of events we use a more conservative volume that is the cone with the vertex in a target pointing to the 5 m-diameter circle *at the end of the fiducial volume.* Thus, we select the hidden photons with momenta inside that cone, which means

$$\frac{|p_\perp|}{p_\parallel} < \frac{2.5}{60+50} \equiv \theta_0. \tag{14}$$

We apply this cut to the momenta of hidden photons produced via bremsstrahlung. The corresponding restriction on momentum space refers to $f_{\rm fiducial}$ in (4).

For the proton channel one integrates the differential flux (2) with $w_{\rm det}$ over the region limited by (14). The number of A' decays in the detector is then given by

$$N_{\rm sig} = N_{\rm POT}\frac{\sigma_{pp}(s)}{\sigma_{pp}(s')}\int dz dp_\perp^2\, w_{ba}(z,p_\perp^2) w_{\rm det} f(z,p_\perp^2), \tag{15}$$

where $f(z,p_\perp^2)$ is defined in eq. (4). We assume that the total number of protons on target will be $N_{\rm POT} = 10^{20}$. The expected number of events is shown in Fig. 3 (left panel). The feature at 0.8 GeV is due to the ω-meson peak in ratio (11).

To roughly estimate contribution of secondary protons we assume that their average energy is (400 GeV/multiplicity) and apply the same procedure described above.

B. Monte Carlo simulation

A proton hitting the target initiates a shower of secondary particles inside the target and muon dump. To precisely account for energy and angular distributions of secondaries, we simulate both the hadronic and the electromagnetic component of the showers. We use the Geant4 simulation toolkit [17] for this purpose.

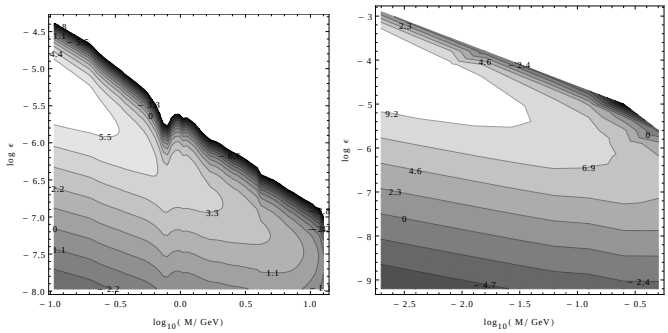

FIG. 3. The $\log_{10}$ of expected number of A' in the detector fiducial volume: proton bremsstrahlung (*left panel*) and meson decays (*right panel*). For the proton contribution we set the Dirac form factor to unity.

Since the SHiP muon dump design is under discussion we choose the most simple geometry for the proton target and muon dump: rectangular parallelepiped of $40 \times 40\,{\rm cm}^2$ front section and 60 m length, made of tungsten. Protons of 400 GeV are directed to the target.

We set Geant4 standard options for particle lists and electromagnetic processes. The only essential choice is the selection of the inelastic hadronic processes generator. We apply 2 recomended options—FTFP_BERT (FRITIOF model) and QGSP_BIC (quark gluon string model)—and find significant difference in both proton interacton cross section and the energy-angular dependence of produced secondary particles. We compare the inclusive cross section with ref. [18] and accept the usage of the QGSP_BIC model.

Cases of short-lived and long-lived particles are processed differently as follows:

- for each meson produced in the program we save its type (π^0, ρ^0 or η), and its 3-momentum p, which is the energy and angle to beam axis θ_z;
- for leptons we fill in the histograms with the total lengths of the tracks of the particles with given energy E_0: $L(E_0) = \sum \Delta l(E{=}E_0, \theta{\le}\theta_0)$, where the sum runs over all segments $\Delta l(E,\theta)$ of all tracks of the particles in the shower inside the material. We chose binning $0 \ldots 400$ GeV with bin step 0.5 GeV. In this way we get four distinct histograms for μ^+, μ^-, e^+, e^- shown in Fig. 4.

To accelerate simulation we apply cut $p > 0.01$ GeV to all particles. To estimate the dark photon rates, 160K of primary protons have been generated.

C. Analysis

Using distributions described above, we calculate the number of signal events inside the detector. For the

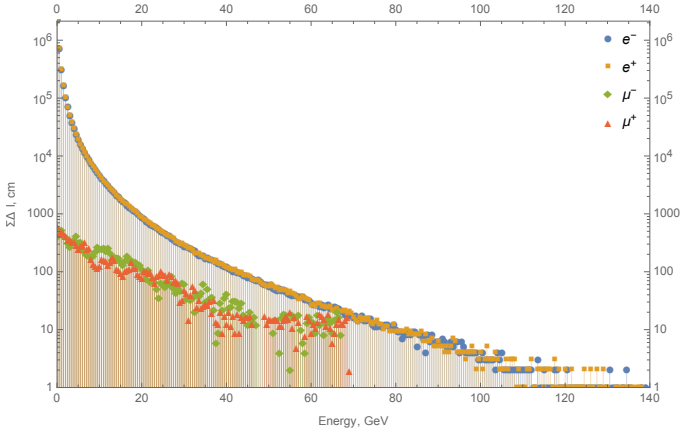

FIG. 4. The overall length of tracks of the particles with energies in a given bin. Result of 160 000 protons on target simulation.

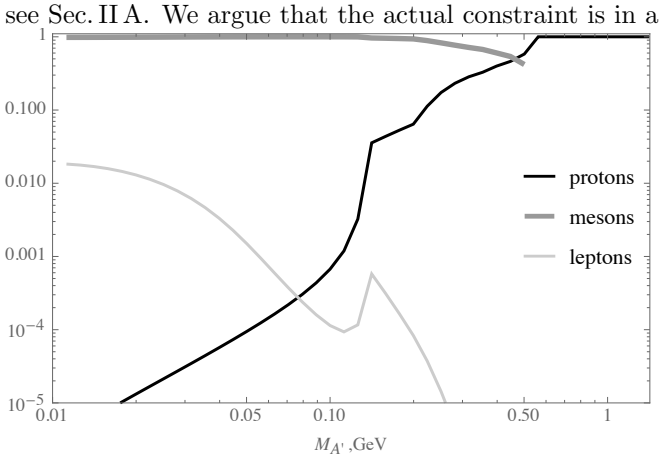

FIG. 5. The partial contribution of proton, meson and electron channels to the total number of events. The kinks on the proton and electron lines near the pion mass correspond to the kinematic cut of the pion branching ratio.

meson channel the number of events is simply $N_{sig} = \sum_p N_m(p)\,\mathrm{Br}(m \to A'X) w_{det} C_{cut}$, where p is the meson momentum, m stands for meson type, e.g. π^0, η^0, $N_m(p)$ is the amount of mesons with given 3-momentum, Br is defined in (8), (9). The Momentum-dependent numerical coefficient C_{cut} accounts for the fraction of A' traveling through the fiducial volume. In N_m we count only mesons with $\theta_z < \theta_0$. The resulting number of signals is presented in Fig. 3.

For secondary electrons propagating in the dump medium one estimates the number of produced hidden photons as

$$\mathcal{N} \simeq n_a \sum_{E_0} \sigma_{forward} L(E_0), \tag{16}$$

where n_a is the nuclei number density, $\sigma_{forward}$ is the differential cross section (5) integrated with respect to the geometry constraint, and E_0 is the electron energy.

Using this distribution we calculate the number of A' decays inside the detector. Partial contributions of the proton, lepton and meson channels to the signal event number are shown in Fig. 5. At small masses meson decays dominate. The proton bremsstrahlung channel starts to dominate when $m_{A'} > m_{\eta^0}$ since heavier A' could not be produced in meson decays in sufficient amounts. In the whole mass region the lepton bremsstruhlung contribution is neglidibly small and, hence, omitted.

To define the domain of parameters $m_{A'}$ and ϵ where SHiP will be sensitive to hidden photons we assume 10^{20} POT, neglect background, and adopt the Poisson statistics which tell us that no events while three events are expected implies an exclusion at 95% confidence level. The exclusion limits are shown in Fig. 1. The dotted black line outlines proton contributions of initial and secondary protons, while solid black line refers to the conservative constraint accounting for the Dirac form factor of proton, see Sec. II A. We argue that the actual constraint is in a region between the dotted and solid lines. As shown in Sec. III, the dark photon lifetime is proportional to ϵ^{-2}, thus, the upper border of the region in Fig. 1 corresponds to a quick decay of the dark photon. For the values of ϵ above the upper line, the hidden photons decay within the shielding. The lower border of the region corresponds reciprocally to a slow decay.

V. DISCUSSION

To summarize, we have estimated the hidden photon signal rate expected in the SHiP experiment, and outlined the region in model parameter space (see Fig. 1), where three paraphoton decays in a 50 m-length detector are expected for each 10^{20} protons on target. The results are rather *conservative* and may be improved by taking into account: *(i)* ρ, ω and other short-lived hadron contributions to hidden photon production via decay, *(ii)* $\pi^{\pm}$ and other long-lived hadron contributions to hidden particle production via bremsstrahlung, *(iii)* quark bremsstrahlung contribution. However, since the number of signal events scales with mixing as ϵ^4, we expect no significant change in our results. As the next steps, the real experiment geometry, detection efficiency, and background events must be analyzed to find the sensitivity of SHiP to the hidden photon models.

We thank W. Bonivento, A. Golutvin, R. Lee, N. Serra and M. Shaposhnikov for useful discussions. This work has been supported by Russian Science Foundation grant 14-22-00161.

[1] http://ship.web.cern.ch, .

[2] W. Bonivento, A. Boyarsky, H. Dijkstra, U. Egede, M. Ferro-Luzzi, *et al.*, (2013), arXiv:1310.1762 [hep-ex].

[3] S. Gninenko, D. Gorbunov, and M. Shaposhnikov, Adv.High Energy Phys. **2012**, 718259 (2012), arXiv:1301.5516 [hep-ph].

[4] A. Boyarsky, O. Ruchayskiy, and M. Shaposhnikov, Ann.Rev.Nucl.Part.Sci. **59**, 191 (2009), arXiv:0901.0011 [hep-ph].

[5] D. Gorbunov and M. Shaposhnikov, JHEP **0710**, 015 (2007), arXiv:0705.1729 [hep-ph].

[6] S. Gninenko, Phys.Lett. **B713**, 244 (2012), arXiv:1204.3583 [hep-ph].

[7] S. Andreas, C. Niebuhr, and A. Ringwald, Phys.Rev. **D86**, 095019 (2012), arXiv:1209.6083 [hep-ph].

[8] J. Blmlein and J. Brunner, Phys.Lett. **B731**, 320 (2014), arXiv:1311.3870 [hep-ph].

[9] M. Pospelov, A. Ritz, and M. B. Voloshin, Phys.Lett. **B662**, 53 (2008), arXiv:0711.4866 [hep-ph].

[10] K. Olive *et al.* (Particle Data Group), Chin.Phys. **C38**, 090001 (2014).

[11] K. J. Kim and Y.-S. Tsai, Phys.Rev. **D8**, 3109 (1973).

[12] J. Arrington, C. Roberts, and J. Zanotti, J.Phys. **G34**, S23 (2007), arXiv:nucl-th/0611050 [nucl-th].

[13] M. Gockeler, P. Hagler, R. Horsley, Y. Nakamura, D. Pleiter, *et al.*, PoS **LAT2006**, 120 (2006), arXiv:hep-lat/0610118 [hep-lat].

[14] J. D. Bjorken, R. Essig, P. Schuster, and N. Toro, Phys.Rev. **D80**, 075018 (2009), arXiv:0906.0580 [hep-ph].

[15] T. Beranek and M. Vanderhaeghen, Phys.Rev. **D89**, 055006 (2014), arXiv:1311.5104 [hep-ph].

[16] B. Batell, M. Pospelov, and A. Ritz, Phys.Rev. **D80**, 095024 (2009), arXiv:0906.5614 [hep-ph].

[17] S. Agostinelli *et al.*, NIM A **506**, 250 (2003).

[18] M. Aguilar-Benitez, W. Allison, A. Batalov, E. Castelli, P. Cecchia, *et al.*, Z.Phys. **C50**, 405 (1991).